Molecular Human Reproduction, Vol.17, No.11 pp. 679–692, 2011
Advanced Access publication on June 22, 2011 doi:10.1093/molehr/gar047

MHR Basic science of reproductive medicine

ORIGINAL RESEARCH

Development of ovarian hyperstimulation syndrome: interrogation of key proteins and biological processes in human follicular fluid of women undergoing *in vitro* fertilization

Karla Jarkovska[1], Helena Kupcova Skalnikova[1], Petr Halada[2], Rita Hrabakova[1], Jiri Moos[3,4], Karel Rezabek[4], Suresh Jivan Gadher[1,5], and Hana Kovarova[1,*]

[1]Department of Reproductive and Developmental Biology, Institute of Animal Physiology and Genetics AS CR, v.v.i., 277 21 Libechov, Czech Republic [2]Laboratory of Molecular Structure Characterisation, Institute of Microbiology AS CR, v.v.i., 142 00 Prague, Czech Republic [3]Sigma-Aldrich spol. s.r.o., 186 00 Prague, Czech Republic [4]Centre of Assisted Reproduction, Department of Obstetrics and Gynaecology, General Teaching Hospital, 128 51 Prague, Czech Republic [5]Merck Millipore, 15 Research Park Drive, St. Charles, MO 63304, USA

*Correspondence address. Tel: +420-315-639-582; Fax: +420-315-639-510; E-mail: kovarova@iapg.cas.cz

Submitted on March 10, 2011; resubmitted on June 7, 2011; accepted on June 14, 2011

ABSTRACT: Ovarian hyperstimulation syndrome (OHSS) is an iatrogenic complication and potentially life-threatening condition resulting from excessive ovarian stimulation during assisted reproductive technologies. Our aim was to identify candidate proteins in follicular fluid (FF) using various proteomic approaches which may help to identify patients at risk of OHSS. We analysed the proteome alterations in FF from patients suffering from severe forms of OHSS (OHSS+) compared with a control group of women without or with only mild signs of OHSS (OHSS−). The 12 abundant proteins of FF were removed using an immunoaffinity system. Pools of remaining depleted proteins were applied to the two-dimensional (2D) electrophoresis and 2D liquid chromatography and proteins in differentially expressed protein spots/fractions were identified by mass spectrometry. Among a total of 19 candidate proteins differentially expressed ($P < 0.05$) between OHSS+ and OHSS− FF samples, three proteins, namely ceruloplasmin, complement C3 and kininogen-1, were found using both 2D techniques. Computer modelling highlighted the important role of kininogen-1 as an anchor for mediated interactions with other identified proteins including ferritin light chain and ceruloplasmin, hepatocyte growth factor-like protein, as well as complement C3 and gelsolin, thus linking various biological processes including inflammation and angiogenesis, iron transport and storage, blood coagulation, innate immunity, cell adhesion and actin filament polymerization. The delineation of such processes may allow the development of informed corrective therapeutic intervention in patients at risk of OHSS and a set of key proteins of the FF may be helpful as potential biomarkers for monitoring IVF therapy.

Key words: biomarkers / computer modelling / human follicular fluid / ovarian hyperstimulation syndrome / proteomics

Introduction

There are millions of couples around the world battling infertility and experts are reporting a steady increase in the number of people who are affected by this problem. International estimates of infertility prevalence and demand for infertility medical care highlight a depressing picture showing a 9% prevalence of infertility (of 12 months) with 56% of couples seeking medical care (Boivin *et al.*, 2007). Such couples, having difficulties conceiving, resort to assisted reproductive technology (ART) such as IVF followed by embryo transfer into the woman's uterus. Results of treatments using ARTs indicated that for IVF, the values of the clinical pregnancy rates per follicle/oocyte aspiration and per embryo transfer in 2006 in Europe were 29.0 and 32.4%, respectively (de Mouzon *et al.*, 2010). Although there was a significant increase in

the reported number of ART cycles and fewer embryos were transferred per treatment in Europe, there was only marginal increase in pregnancy rates as well as only minor reduction in multiple deliveries as observed in 2005 and 2006 (Andersen et al., 2009; de Mouzon et al., 2010).

Controlled ovarian hyperstimulation is a key factor in the success of IVF. Since human chorionic gonadotrophin (hCG)—a common substitute for natural LH in IVF cycles —is widely used, many studies have been carried out to assess its implication (Lei et al., 1992; Rao et al., 1993; Albert et al., 2002). The resultant evidence suggested that hCG played a significant role in the development of ovarian hyperstimulation syndrome (OHSS; Wulff et al., 2000). The onset of this iatrogenic complication usually occurs during luteal phase in ovulation stimulation or during early pregnancy with prevalence between 0.5 and 1.5% of all IVF cycles (Andersen et al., 2009; de Mouzon et al., 2010). OHSS presents itself in various forms from mild stage (33%) to moderate (3–6%) to severe disease state (0.1–3%); the latter can be highly complicated, may be fatal and definitely requires intensive care management (Nastri et al., 2010).

The main symptom of OHSS is cystic enlargement of ovaries and fluid leakage from the intravascular space due to increased permeability and ovarian neoangiogenesis (Gerris et al., 2006). Subsequently, such an increase in the capillary permeability of the ovaries and mesothelial surfaces can lead to massive ascites, pleural effusion and occasionally even pericardial effusion. Severe forms of OHSS are also accompanied by electrolyte and hemodynamic disturbances (Chen et al., 2008) resulting in thrombosis (Chipwete et al., 2009) or renal failure (Merrilees et al., 2008). Unfortunately, prediction and diagnosis mostly involves measurement of blood estradiol levels and number of growing follicles which is certainly not sufficient and treatment strategies remain symptomatic without any specific treatment for OHSS. Hence, an accurate and reliable investigative approach is needed for early prognosis/diagnosis and prompt prevention. Possibility of utilizing a protein or a set of proteins present in the follicular fluid (FF) of patients which constitutes the *in vivo* environment of the oocyte as potential biomarker(s) was highlighted by Gadher et al. (2009). FF representing the intrafollicular milieu is easily accessible as a resultant by-product during aspiration of oocytes from mature ovarian follicle (Fortune, 1994) and certain proteins observed here may be contributory to development of OHSS.

Previously, we used a proteomic approach and showed involvement of innate immune function of complement cascade in FF of women undergoing controlled ovarian hyperstimulation for IVF. Low complement activity and the presence of C-terminal fragment of perlecan suggested possible links to angiogenesis, which is a vital process in physiological folliculogenesis and placental development. Differences in proteins associated with blood coagulation were also found in the follicular milieu (Jarkovska et al., 2010). In this study, the proteome alterations in FF which might be associated with the development of OHSS were analysed utilizing samples of FF from patients suffering from severe form of OHSS (patient group; OHSS+) compared with control group of women without or with only mild signs of OHSS (control group; OHSS−). We used a combination of several proteomic techniques to obtain two-dimensional (2D) protein profiles of FF samples as well as to access important middle and low abundant proteins. First, 12 abundant proteins of FF were removed using the IgY-12 immunoaffinity system. Pools of remaining depleted proteins were then applied to the 2D electrophoresis (2-DE) and 2D liquid chromatography (2D LC). The resulting 2D protein maps were evaluated using software tools and protein spots/fractions with significant increase or decrease in FF from OHSS+ group compared with OHSS− group of women were subjected to protein identification by mass spectrometry (MS). Selected protein changes were further verified by independent immunoblotting (Fig. 1) and computer modelling was used to reveal protein interaction network integrating severe OHSS related proteins to help judge the severity of the onset.

Materials and Methods

Chemicals

IgY-12 High Capacity LC 10 Proteome Partitioning kit and ProteomeLab^{TM} PF 2D kit (includes chromatofocusing column, high-resolution reverse-phase column, start buffer, eluent buffer and PD-10 columns) were purchased from Beckman Coulter (Fullerton, CA, USA). Amicon Ultra-15 Centrifugal Filter Device was from Millipore (Bedford, MA, USA). Acrylamide, bis-acrylamide, urea, Tris-base, thiourea, sodium dodecyl sulphate (SDS), bromophenol blue, amonium persulfate (APS), tetramethylethylenediamine (TEMED), n-octyl glucoside, Tris(2-carboxyethyl)phosphine hydrochloride (TCEP), iminodiacetic acid and trifluoroacetic acid (TFA) were obtained from Sigma (St. Louis, MO, USA). Nonidet-40, 3-[(3-cholamidopropyl)dimethylammonio]-1-propanesulfonate (CHAPS) and dithiothreitol (DTT) were from USB Corporation (Cleveland, OH, USA). Glycerol and β-glycerolphosphate were purchased from Serva Electrophoresis GmbH (Heidelberg, Germany). Protease inhibitors cocktail was obtained from Roche (Basel, Switzerland). Immobiline DryStrip (18 cm, 4–7) and ampholytes pH 4–7 were purchased from GE Healthcare (Uppsala, Sweden). Sypro Ruby Protein Gel Stain was from Bio-Rad Laboratories (Hercules, CA, USA). All other chemicals for protein fractionations and silver staining were of HPLC or analytical grade and buffers were prepared using Milli-Q water system (Millipore Bedford, MA, USA). Unless otherwise specified, all chemicals used for MS were from Sigma (Steinheim, Germany).

Female patients and collection of FF

Women undergoing controlled ovarian hyperstimulation for IVF were recruited for the study at the Centre of Assisted Reproduction, Department of Obstetrics and Gynecology, General Teaching Hospital in Prague. All female patients gave their informed consent prior to sample collection.

To achieve stimulation, standard treatment protocol was applied including controlled ovarian FSH hyperstimulation using GnRH short antagonists or GnRH long agonists with hCG administration to induce oocyte maturation. Oocyte transvaginal retrieval was performed 36 h after hCG administration according to the strict procedure approved by the Centre of Assisted Reproduction. Each FF sample was obtained from puncture of dominant ovarian follicles (in diameter from 14 to 22 mm). Only macroscopically clear fluids, indicating lack of contamination, were considered in the study. After oocyte isolation, FF was centrifuged to remove cellular components and debris and then transferred to sterile polypropylene tubes and frozen at −70°C until further analysis (Moos et al., 2009).

Samples were obtained from a total number of 31 women (average BMI 23.25 ± 4.19; average age 30.07 ± 3.19; average number of follicles 28.16 ± 9.37) and were separated into two groups: (i) OHSS+ patient group including 13 women (average BMI 22.94 ± 4.37; average age 29.46 ± 3.60; average number of follicles 29.84 ± 6.30) suffering from severe form of OHSS characterized by massive ascites,

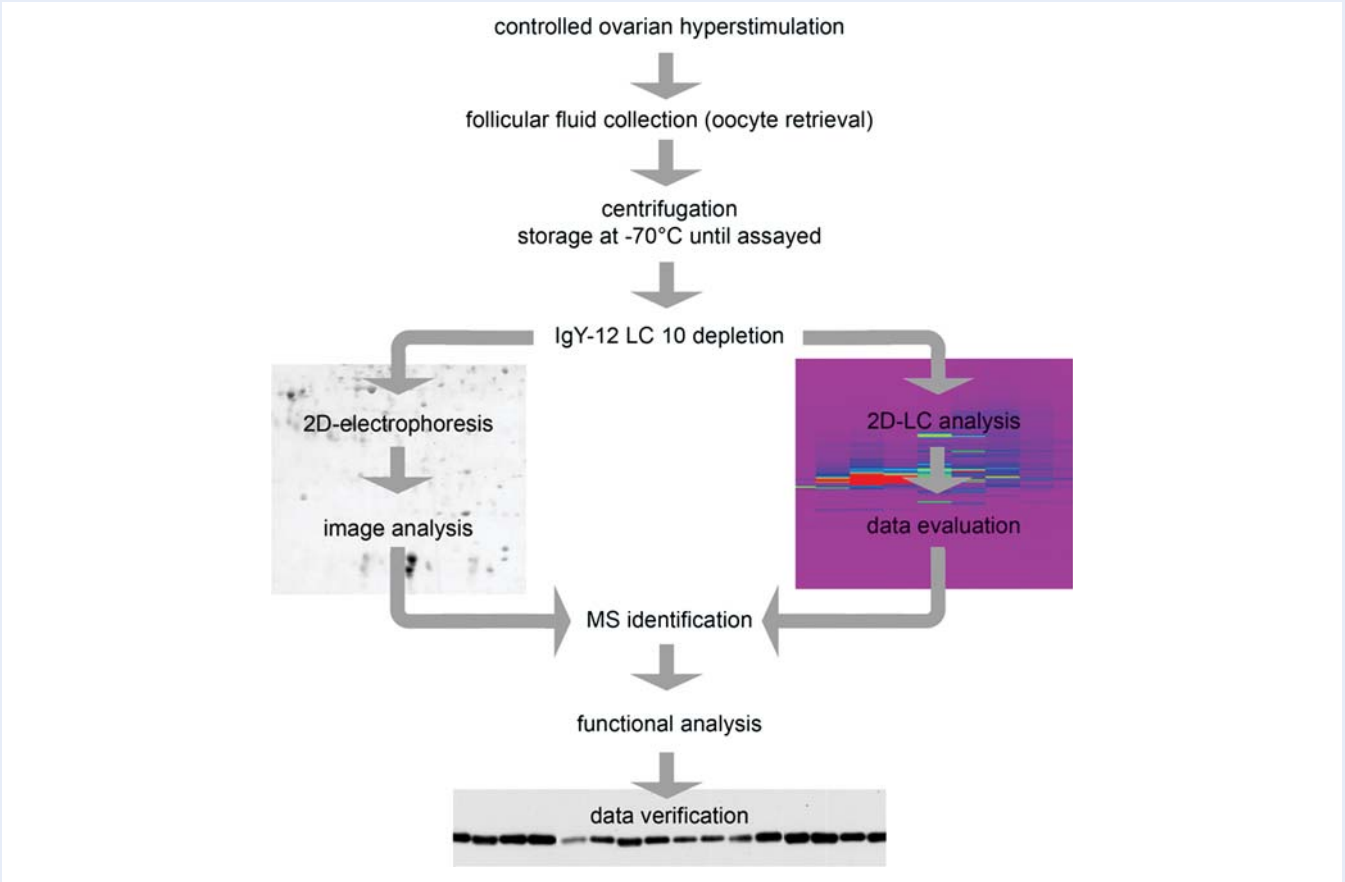

Figure 1 Schematic presentation of the IgY-12, 2-DE and 2D LC workflows. Samples of FF were retrieved from women undergoing controlled ovarian stimulation and were depleted of the 12 most abundant plasma/human FF matched proteins and processed for 2-DE and 2D HPLC analyses as indicated in the workflows. Subsequently, proteomic data were verified by immunoblotting and computer modelling was used to reveal protein interaction network integrating OHSS discriminating proteins.

haemoconcentration (hematocrit > 45%, WBC > 15 000/ml), oliguria, creatinine > 130 m mol/l, creatinine clearance < 50 ml/min and enlarged ovaries (>5 cm); (ii) OHSS− control group consisting of 18 women (average BMI 23.47 ± 4.17; average age 30.53 ± 2.87; average number of follicles 26.94 ± 11.10) either without any symptoms of OHSS or with only mild form presented by bloating, nausea, abdominal distention and sonography-determined size of ovaries <5 cm (Navot *et al.*, 1992). Both groups were matched as to BMI, age and number of growing follicles. Additionally, around 39% of all IVF cycles resulted in successful pregnancy without any significant difference between OHSS+ and OHSS− groups of women.

The distribution of the samples with reference to applied proteomic technologies is graphically illustrated in Fig. 2: 9 samples of FF (4 OHSS+ patients and 5 OHSS− controls) were applied to 2-DE, whilst 12 FF samples (6 OHSS+ patients and 6 OHSS− controls) were analysed using 2D LC. Of all the samples, 6 were shared and analysed using both proteomic techniques. For independent verification of proteomic findings, a set of 23 samples were used (11 OHSS+ patients and 12 OHSS− controls) of which 7 were included in 2D LC fractionation. Four of all samples were processed using all approaches applied in this study.

Depletion of major abundance proteins

Depletion of the 12 abundant plasma matched proteins (albumin, IgG, transferrin, fibrinogen, IgA, α2-macroglobulin, IgM, α1-antitrypsin,

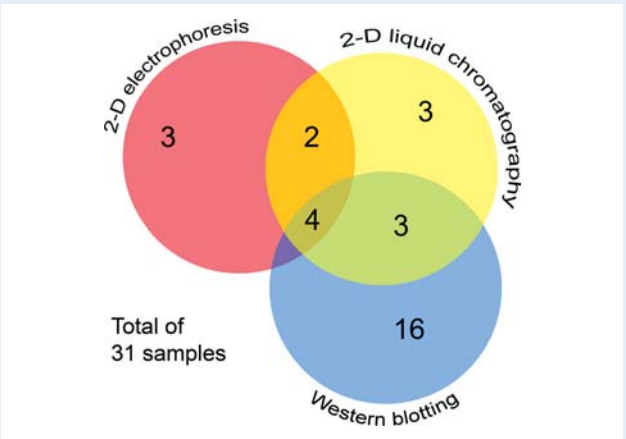

Figure 2 The distribution of the samples among applied proteomic technologies. Nine samples of FF (4 OHSS+ patients and 5 OHSS− controls) were applied to 2-DE, whilst 12 FF samples (6 OHSS+ patients and 6 OHSS− controls) were analysed using 2D LC. For western blot, a set of 23 samples were used (11 OHSS+ patients and 12 OHSS− controls).

haptoglobin, α1-acidic glycoprotein and apolipoproteins A-I and A-II) present in FF (Shalgi et al., 1973; Huang et al., 2005) was carried out using multiple immunoaffinity ProteomeLab IgY-12 LC10 column (binding capacity equal to 250 μl of blood plasma; Beckman Coulter, Fullerton, CA, USA) as described previously (Jarkovska et al., 2010). Protein concentration of samples was measured at first using a BCA protein assay kit (Thermo Scientific, Rockford, IL, USA). Aliquot of FF sample containing 20 mg of proteins was diluted to final volume of 750 μl using dilution buffer containing 10 mM Tris–HCl, 0.15 M NaCl, pH 7.4. The diluted sample was filtered through a 0.45 μm membrane using spin filters provided in IgY-12 LC 10 kit, loaded on IgY-12 LC 10 column and standard LC protocol provided by manufacturer was carried out. Flow-through fractions from six cycles of the each individual FF sample were then pooled, concentrated on Amicon Ultra—15 centrifugal filter devices to approximate volume 0.5 ml and diluted in denaturation buffer (7.5 M urea, 2.5 M thiourea, 12.5% glycerol, 62.5 mM Tris–HCl, 2.5% *n*-octylglucoside, 1.25 mM EDTA) for 2D LC and 2-DE.

Two-dimensional electrophoresis and image analysis

Sample aliquots corresponding to 250 and 500 μg of FF depleted proteins were precipitated by addition of 0.15% sodium deoxycholate for 10 min and 72% trichloroacetic acid for 30 min (both in 1/10 of total volume) with 80% yield in average thus providing 200 and 400 μg of proteins to be loaded on 2-DE. After washing with ice-cold acetone, pellets were resolubilized in 150 μl of the sample buffer containing 9 M urea, 3% (w/v) CHAPS, 2% (v/v) Nonidet 40, 70 mM DTT, pH 4–7 ampholytes (0.5% w/v), 10 mM β-glycerol phosphate, 5 mM sodium fluoride, 0.1 mM sodium orthovanadate and protease inhibitors. After 30 min of resolubilization at room temperature, samples were loaded on the first dimension isoelectric focusing (IEF) separation using active in gel rehydration at 50 V of Immobiline DryStrips (IPG strip 18 cm 4–7) in rehydration buffer containing 7 M urea, 2 M thiourea, 4% CHAPS, pH 4–7 ampholytes (2% w/v), 1 mM β-glycerol phosphate, 5 mM sodium fluoride, 1 mM sodium orthovanadate, 1× protease inhibitors cocktail (Roche) and 0.003% bromophenol blue. 2-DE was performed as described previously (Jarkovska et al., 2010). Briefly, IEF was performed on IEF Cell (Bio-Rad, Hercules, CA, USA) system. After IEF separation the gel strips were equilibrated in 50 mM Tris–HCl, pH 6.8, 6 M urea, 30% glycerol, 4% SDS, 1.2% (v/v) DeStreak reagent and bromophenol blue for 20 min and applied to vertical 12% SDS–PAGE (180 × 180 × 1 mm gel). Gels were then stained with MS compatible fluorescent dye Sypro Ruby. Stained gels were scanned and digitized at 800 dpi resolution using a Pharos FX scanner (Bio-Rad, Hercules, CA, USA). The images were evaluated using Imagemaster 2D Platinum version 6.0 software (GE Healthcare, Uppsala, Sweden). The evaluation was done separately for protein images corresponding to the lower load of 200 μg depleted FF proteins with 4 OHSS+ patient and 4 OHSS− control samples, and higher load of 400 μg of depleted FF proteins including 3 OHSS+ patient and 3 OHSS− control samples. After automatic spot detection and matching, manual editing was performed and the results were in good agreement with those from visual inspection. Data were normalized, i.e. expressed as relative intensity of all valid spots, analysed using Student *t*-test available within the Imagemaster 2D Platinum software, and the protein spots with statistically different expression (*P*-value of ≤ 0.05) in the two types of samples were selected for identification by MS. The gels were re-stained using silver staining according to the protocol published by Shevchenko et al. (1996) and were stored at 4°C in 10% MeOH.

Two-dimensional ProteomeLab PF 2D chromatography and image analysis

Samples of depleted FFs in denaturating buffer were loaded on a PD10 column equilibrated with 25 ml of the PF 2D start buffer to exchange denaturating lysis buffer with start buffer. The total protein concentration in the sample collected from PD 10 column was determined by direct measurement of absorbance at 280 nm (DU 7400 spectrophotometer, Beckman, Fullerton, CA, USA). Fractionation of the proteins on 2D LC was performed as described previously (Jarkovska et al., 2010). For the first dimension, chromatofocusing fractionation (HPCF) using two buffers, a start buffer pH 8.55 and an elution buffer pH 4.0, to generate an internal linear pH gradient on the column, was utilized. The proteins remaining on the HPCF column at pH 4.0 were washed out by 1 M NaCl in 30% *n*-propanol solution. UV detection was performed at 280 nm and the pH of the effluent was monitored using a flow-through online pH probe. Fraction collection (pI fractions) started at the beginning of the analysis and individual fractions were collected in 0.3 pH intervals (during the linear pH gradient, started when pH reached 8.3) or with maximum time 8.5 min when the pH did not change. The percentage of protein recovery from the column with pH gradient 8.3–4 was about 45%, while the remaining part of the loaded proteins was collected in either basic (flow-through) or acidic (wash out) fractions. The pI fractions containing any proteins detected at 280 nm were further separated on reversed phase column packed with non-porous silica beads (HPRP). Solvent A was 0.1% trifluoracetic acid (TFA) in water and solvent B 0.08% TFA in acetonitrile (MeCN). The separation was performed at 50°C at a flow rate 0.75 ml/min. The gradient was run from 0 to 100% B in 30 min, followed by 100% B for 4 min and 100% A for 10 min for re-equilibration of the column. UV absorption was monitored at 214 nm. The fractions were collected in 0.13 min time intervals into 96-deep well plates using the fraction collector Gilson FC204 (Immunotech, a.s. Prague, Czech Republic) and stored at −80°C until further use.

2D protein expression maps of FF samples displaying pH corresponding to protein isoelectric point (pI) versus protein hydrophobicity were generated by ProteoVue software running on PF 2D system. The Viper software version 2.3.0.0 (Ludesi, Malmö, Sweden) was used for PF 2D data evaluation of protein maps of 6 OHSS+ patient samples and 6 OHSS− controls. The profiles of the second dimension were matched, normalized and quantitative data were analysed using analysis of variance implemented in Viper software. Only statistically significant (*P*-value of ≤ 0.05) and reproducible protein peaks were selected for follow-up protein identification using MS.

Enzymatic digestion, MALDI MS and protein identification

Tryptic digestion and MALDI mass spectrometric identification of proteins from 2-DE gels were done as described previously (Jarkovska et al., 2010) using SwissProt 2011_01 database. The fractions from 2D-HPLC were dried completely using the SpeedVac concentrator, dissolved in 50 μl of the cleavage buffer containing 25 mM 4-ethylmorpholine acetate, 5% MeCN, and trypsin (5 ng/μl; Promega, Madison, WI, USA), and incubated overnight at 37°C. The digestion was stopped by addition of 7 μl of 5% TFA in MeCN. The aliquot (0.5 μl) of the resulting peptide mixture was deposited on the MALDI target and allowed to air-dry at room temperature. After complete evaporation, 0.5 μl of MALDI matrix solution (α-cyano-4-hydroxycinnamic acid in 50% MeCN/0.1% TFA; 5 mg/ml) was added. Mass spectra were measured on the APEX-Qe FTMS instrument equipped with a 9.4 T superconducting magnet and a Combi ESI/MALDI ion source (Bruker Daltonics, Billerica, MA, USA). The spectra were acquired in the mass range of 650–3500 kDa and calibrated

internally using the monoisotopic $[M+H]^+$ ions of trypsin autoproteolytic fragments. The peak lists in mgf data format were created using DataAnalysis 4.0 program (Bruker Daltonics) with SNAP peak detection algorithm. The peak lists were searched using ProFound search engine (http://prowl.rockefeller.edu/prowl-cgi/profound.exe) against IPI human database (2010/02/01) with the following search settings: peptide tolerance of 3 ppm, missed cleavage site value set to one, variable oxidation of methionine and protein N-term acetylation.

Immunoblot and quantitative analysis

Aliquots of the total protein extracts of non-depleted FF corresponding 5 μg were separated in 10% SDS–PAGE gels (except for ceruloplasmin where 6% gels were used) using Mini PROTEAN® 3 system (Bio-Rad, Hercules, CA, USA). Proteins were then transferred to Immobilon P (Millipore, Bedford, MA, USA) membranes using a semidry blotting system (Biometra, Göttingen, Germany) and transfer buffer containing 48 mM Tris, 39 mM glycine and 20% methanol (except for ceruloplasmin, where 10% MeOH was used). The membranes were blocked for 1 h with 5% skimmed milk (except for ceruloplasmin, where 3% milk was used) in Tris-buffered saline with 0.05% Tween 20 (TBST, pH 7.4) and incubated overnight with primary antibodies specific for apolipoprotein A-IV (Sigma Aldrich, St. Louis, MO, USA; HPA001352; 1:10 000), kininogen-1 (Sigma Aldrich, St. Louis, MO, USA; HPA001616; 1:5000), ceruloplasmin (Abcam, Cambridge, MA, USA; ab51083; 1:10 000) and α-2-HS-glycoprotein (fetuin-A, Santa Cruz Biot., CA, USA; sc-28924; 1:20 000). Peroxidase-conjugated secondary anti-rabbit or anti-mouse IgG antibodies (Jackson Immunoresearch, Suffolk, UK) were diluted 1:10 000 (except for fetuin-A, where 1:100 000 dilution was used) in 5% skimmed milk in TBST, and the ECL+ chemiluminiscence (GE Healthcare, Uppsala, Sweden) detection system was used to detect specific proteins. The exposed CL-XPosure films (Thermo Scientific, Rockford, IL, USA) were scanned by a calibrated densitometer GS-800 (Bio-Rad, Hercules, CA, USA). The proteins bands of each sample were quantified as Trace Quantity (the quantity of a band as measured by the area under its intensity profile curve, units are intensity × mm) using Quantity One software (Bio-Rad, Hercules, CA, USA). The total protein load was checked visually using silver staining of the membranes after immunodetection.

Computer modelling of protein network

To analyse functional aspects including possible protein interactions among identified proteins discriminating OHSS and to reveal further as yet unspecified interacting partners, we used an Interologous Interaction Database (I2D; version 1.8). This database version of both known and predicted protein–protein interactions contained 102 740 source interactions, 59 373 predicted interactions for human and is available online on http://ophid.utoronto.ca/ophidv2.201/. For modelling of the protein interaction network, we entered a list of our identified proteins, except three known highly abundant proteins (alpha-1-antitrypsin, apolipoprotein A-I and serum albumin) in which, despite attempts to deplete completely, trace amounts detectable by MS remained in the samples. In addition, we included in the modelling vascular endothelial growth factor (VEGF), growth factor with recognized importance in human fertility and ovarian function but also implicated in pathogenesis of OHSS when dysregulated (Chen *et al.*, 2010; Rodewald *et al.*, 2009). Search criteria for observing interactions were set to select humans as target organism and graph viewer was set to output format. The final illustration was exported and visualized using NAViGaTOR (Network Analysis, Visualization & Graphing TORonto) software (http://ophid.utoronto.ca/navigator) version 2.1.13. In protein–protein interaction networks, nodes represent proteins and edges between nodes represent physical interactions between the proteins. NAViGaTOR allows nodes to be colour-coded according to Gene Ontology (GO—a controlled vocabulary describing properties of genes; http://www.geneontology.org/) terms.

Results

Depletion of the most abundant proteins of FF for follow-up proteomic analyses

In order to overcome limitations of commonly used proteomic techniques related to high dynamic range of protein concentration in biological fluids and access middle or low abundant proteins (μg/ml–pg/ml), FF samples were depleted of 12 abundant proteins (mg/ml). The immunoaffinity column IgY-12 LC 10 was utilized for this purpose and removal of abundant proteins was monitored using 2-DE fractionation of flow-through and bound fractions (Jarkovska *et al.*, 2010). One cycle provided on average 610 μg of flow-through depleted proteins, which corresponded to removal of 97% of original protein amount (20 mg). In total, six depletion cycles for each sample were necessary to obtain 2 mg of depleted proteins of each individual sample for one run of 2D LC PF 2D analysis and as well as for 2-DE analysis.

Proteomic changes observed in depleted FF of OHSS patients compared with asymptomatic/mild control group using two different approaches: 2D LC and 2-DE

The depleted proteins for 2-DE analysis were precipitated as described above. We decided to analyse two protein loads: (i) the lower dose equal to 200 μg to allow monitoring of middle abundant proteins among depleted FF proteins, most of which are present in the upper part of gel; (ii) the higher dose of 400 μg protein to reveal lower abundant protein spots mainly in the gel region with Mw under 60 kDa. The separation was carried out on gels of the pH 4–7 and Mw 10–200 kDa range and resulted in 674 ± 96 and 1064 ± 191 distinct protein spots for 200 and 400 μg protein loads, respectively (Fig. 3A–D). The statistical comparison between the OHSS+ patients compared with the control OHSS− group revealed 23 and 28 differentially expressed protein spots (*P*-value of ≤0.05) for 200 and 400 μg protein loads, respectively. After considering spot reproducibility and intensity, 19 of these protein spots were chosen for further MS identification and proteins in 16 of them were satisfactorily identified (Supplementary data, Table SI; Fig. 3A–D). Among the 16 quantitatively altered protein spots, nine were decreased in FF of OHSS+ samples (Fig. 3E Nos. 336, 898, 1612, 1843 and F Nos. 2244, 2634, 2896, 2897, 3230) and seven spots were significantly increased (Fig. 3E Nos. 1390, 1438, 1439 and F Nos. 1968, 2102, 2573 and 2666). An abbreviated list of identified differentially expressed proteins and their biological functions is presented in Table I. Supplementary data, Table SI provides comprehensive information about the identified proteins (spot numbers, protein names, database accession numbers, regulations, fold changes, theoretical values of MW and pI, and all MS identification data including Mascot scores, sequence coverage, matched peaks, unmatched peaks and MS/MS confirmation).

The purpose of 2D LC PF 2D experiments was to use an advanced gel-independent fractionation technique which overcomes many of

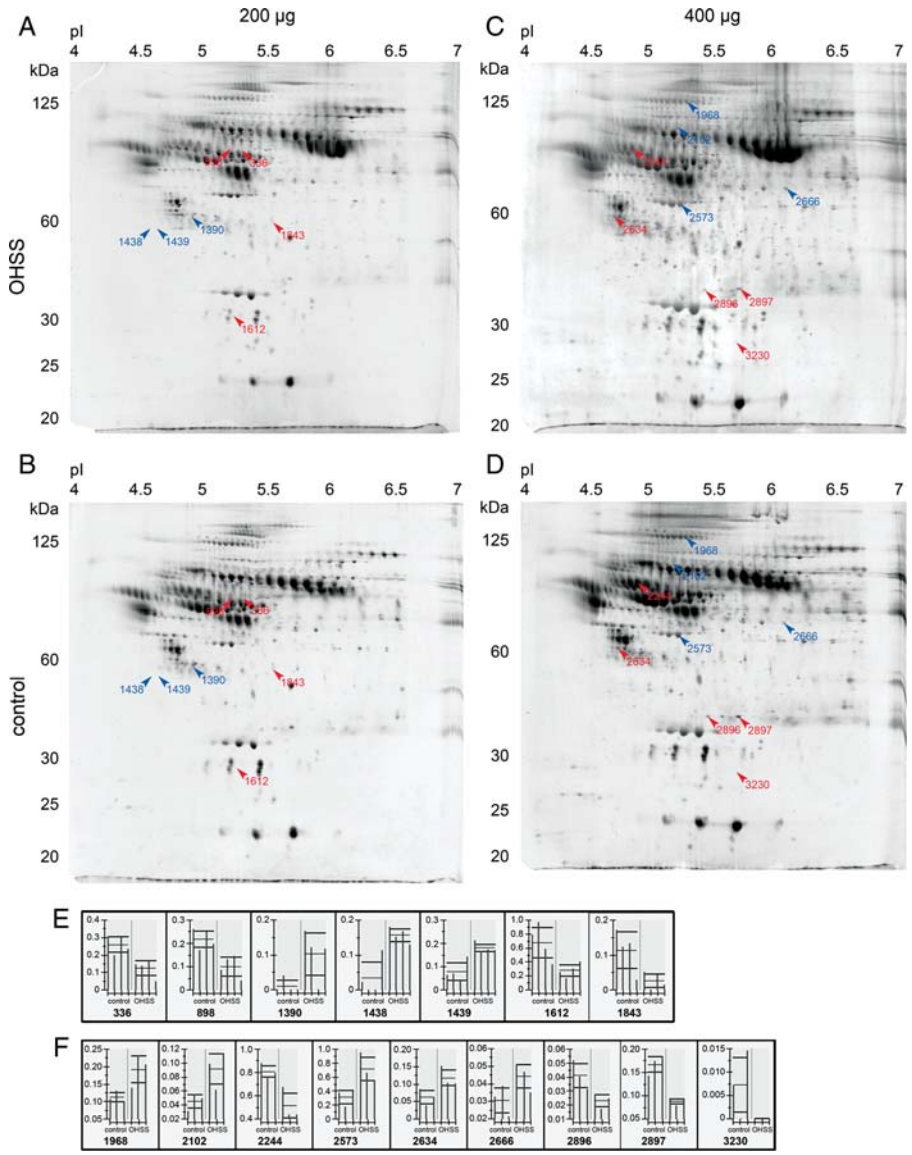

Figure 3 2D electrophoretic protein maps of human FF depleted of the 12 most abundant plasma matched proteins and set of protein spots. Protein lysates of samples of depleted FF were subjected to 2-DE, followed by fluorescent Sypro Ruby staining and image analysis using Imagemaster 2D Platinum version 6.0 software. (**A**–**D**) Representative gels from depleted FF of 200 and 400 µg loads, respectively, and protein spots that were differentially expressed (*P*-value of $\leq$0.05). Regulated proteins are indicated by their spot numbers assigned by the software. Blue numbers indicate higher protein level in FF of OHSS+ samples and red numbers denote lower level in OHSS+ FF compared with control OHSS− samples. (**E** and **F**) Relative volume intensities of identified regulated protein spots calculated and graphically presented by Imagemaster 2D Platinum version 6.0 software. Left columns correspond to control OHSS− FF samples (control) and right columns to OHSS+ FF samples (OHSS).

2-DE drawbacks and allows the fractions of intact proteins to be directly utilized for MS analysis. A typical 2D-LC analysis resulted in separation on average into 1026 protein peaks, which are depicted in the 2D protein map generated using ProteoVue software (Fig. 4). The evaluation of qualitative and quantitative differences between 2D protein maps using Viper software identified 33 differentially expressed protein bands with *P*-value of $\leq$0.05 between the samples representing OHSS+ patients and OHSS− control group. Five of protein peaks with area under curve higher than 1×10^{-5} at 214 nm (which corresponds to the protein amount enough for reliable MS protein identification) and reproducible peak profile were chosen for MS (Fig. 4) and the proteins were satisfactorily identified. All of these protein peaks collected after the second dimension, contained more than one protein and this was re-confirmed by MS analysis. A summary of 2D LC differentially expressed proteins and their functions are presented in Table II. Supplementary data, Table SII provides comprehensive information about the identified proteins (fraction numbers, protein names, database accession numbers, regulations, fold changes, theoretical values of MW and pI, and MS identification data including ProFound Expectation values, sequence coverage and

Table I The list of significantly different proteins identified (*P*-value of ≤0.05) between FF of OHSS+ and OHSS− selected using 2-DE.

Spot No	Protein name	SwissProt No.	MW, kDa	pI	Up-regulation, fold change	Functionality
	200 μ load protein					
336	Gelsolin precursor Ig alpha-1 chain C region	GELS_HUMAN IGHA1_HUMAN	85 38	5.9 6.1	OHSS−, 2.0	Actin filament polymerization Immune response
0898	Gelsolin precursor	GELS_HUMAN	86	5.9	OHSS−, 2.2	Actin filament polymerization
1390	Complement factor I precursor	CFAI_HUMAN	66	7.7	OHSS+, 8.3	Complement activation, classical pathway Innate immune response
1438, 1439	Complement C3 precursor[a]	CO3_HUMAN	187	6.0	OHSS+, 4.7/2.4	Complement activation, alternative pathway Complement activation, classical pathway Positive regulation VEGF production
1612	Retinol-binding protein 4	RET4_HUMAN	23	5.8	OHSS−, 2.2	Glucose homeostasis Positive regulation of immunoglobulin secretion Response to retinoic acid Retinol metabolic process
1843	Inter-alpha-trypsin inhibitor heavy chain H4 precursor[a]	ITIH4_HUMAN	103	6.5	OHSS−, 5.0	Acute-phase response Hyaluronan metabolic process
	400 μ load protein					
1968	Ceruloplasmin precursor	CERU_HUMAN	125	5.4	OHSS+, 2.3	Cellular iron ion homeostasis Copper ion transport Oxidation reduction
2102	Inter-alpha-trypsin inhibitor heavy chain H4 precursor[b]	ITIH4_HUMAN	103	6.5	OHSS+, 2.8	Acute-phase response Hyaluronan metabolic process
2244	Kininogen-1 precursor	KNG1_HUMAN	72	6.3	OHSS−, 3.8	Blood coagulation Inflammatory response Negative regulation of blood Coagulation Negative regulation of cell adhesion Vasodilation
2573	Apolipoprotein A-IV precursor	APOA4_HUMAN	47	5.3	OHSS+, 2.2	Cholesterol homeostasis Chylomicron assembly Innate immune response in mucosa Leucocyte cell−cell adhesion Lipoprotein metabolic process
2634	Complement C3 precursor[a]	CO3_HUMAN	187	6.0	OHSS+, 1.9	Complement activation, alternative pathway Complement activation, classical pathway Positive regulation VEGF production
2666	Pigment epithelium-derived factor precursor	PEDF_HUMAN	46	6.0	OHSS+, 1.35	Cell proliferation Negative regulation of angiogenesis
2896, 2897	Serum amyloid P-component precursor	SAMP_HUMAN	25	6.1	OHSS−, 2.4/3.0	Acute-phase response
3230	Ferritin light chain	FRIL_HUMAN	20	5.5	OHSS−, 7.9	Cellular iron ion homeostasis Iron ion transport Oxidation reduction

The table shows spot number, protein name, SwissProt No., predicted MW and pI, regulation/fold of the change and functionality based on search in UniProt/Gene Ontology/Biological Process.
[a]C-terminal fragment.
[b]N-terminal fragment.

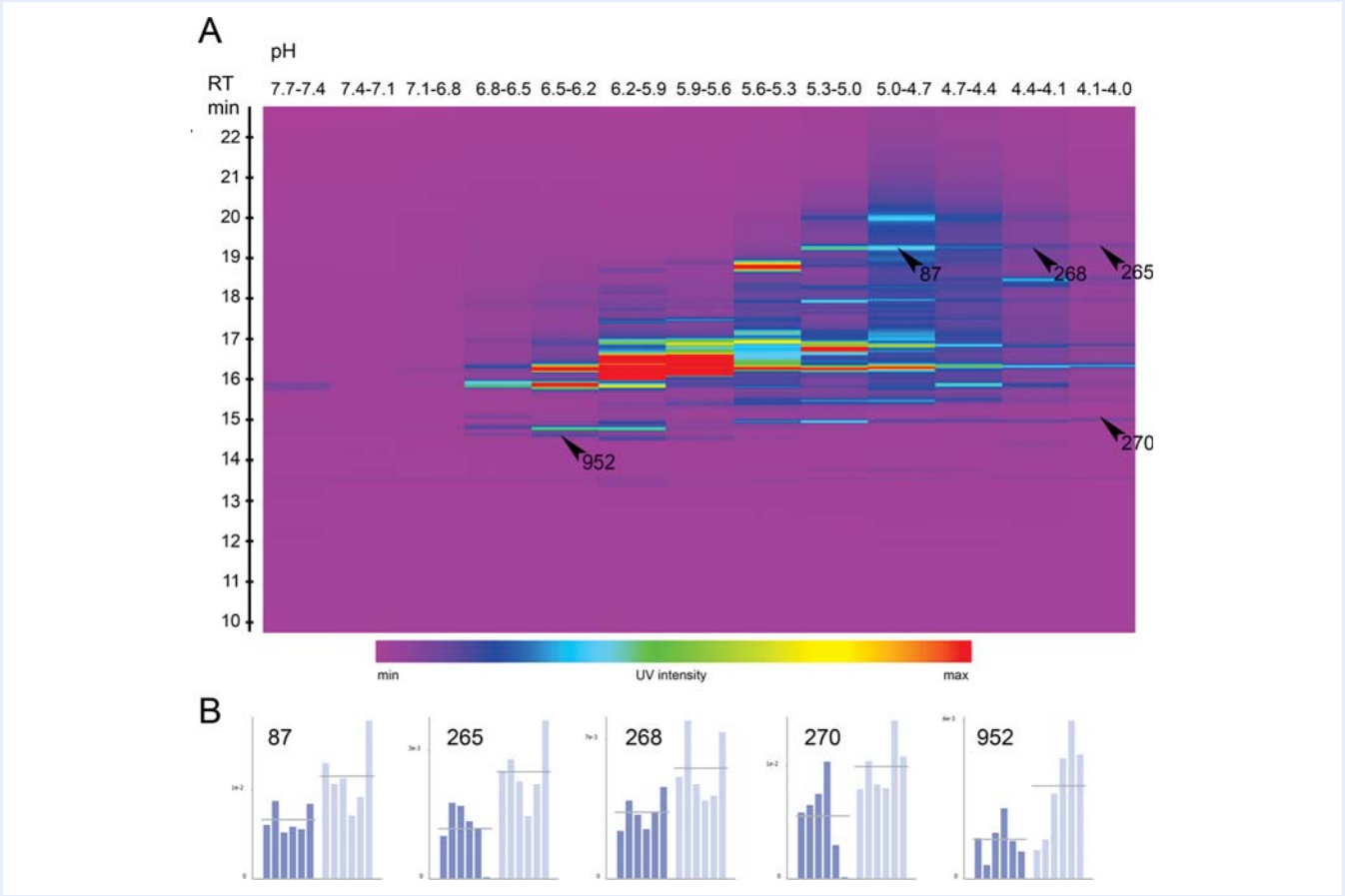

Figure 4 2D liquid chromatography protein map of human FF depleted of the 12 most abundant plasma matched proteins and set of protein bands significantly different significantly different in patients suffering from severe OHSS. Protein lysates of paired samples of depleted FF were subjected to 2D liquid chromatography and protein fractionation/level was monitored using UV detection. 2D protein expression maps were generated by ProteoVue software and their images were evaluated using Viper software. (**A**) Representative protein map from depleted FF and protein bands that were present in significantly different levels (*P*-value of $\leq$0.05) in OHSS+ FF compared with OHSS− FF and were selected for follow-up identification using MS. The colours of the protein bands correspond to UV intensity and provide information about protein quantification. Regulated proteins are indicated by their numbers assigned by Viper software. (**B**) Relative volume intensities of regulated protein bands calculated and graphically presented by Viper software. The left columns correspond to biological replicates of OHSS+ FF and right columns to OHSS− FF.

number of the matched peaks). All of the differentially expressed protein peaks revealed by PF 2D approach and identified were present at a significantly increased level in FF of OHSS+ patient samples (Table II, Fig. 4). Relative differences in expression ranged from 1.67-fold to as much as 2.38-fold. These protein peaks contained non-target proteins such as ceruloplasmin, complement C3, alpha-2-HS-glycoprotein, haemopexin and alpha-1B-glycoprotein and it was demonstrated (Liu *et al.*, 2006) that these proteins may partly bind to IgY-12 affinity column and it occurs in a highly reproducible manner. On the other hand, we found proteins like kininogen-1, complement factor H-related protein 1 and hepatocyte growth factor-like protein, which were typical non-target not bound proteins (Huang *et al.*, 2005; Liu *et al.*, 2006). The presence of alpha-1-antitrypsin, apolipoprotein A-I and albumin is due to incomplete removal of these proteins in the course of depletion of major abundant proteins as the manufacturer guarantees the removal of 95% (for Apo-AI and α-1-antitrypsin) or 99% (for human albumin) of protein amount. The robustness, reproducibility and specificity of the ProteomeLab IgY-12 high abundance protein depletion system were evaluated using human plasma proteome characterization in combination with high resolution LC-MS/MS (Liu *et al.*, 2006). Because the patterns and distribution of the proteins of human FF, similarly to plasma, between bound and flow-through fractions are highly reproducible for the biological replicates of the same sample, such processes most likely do not significantly affect the quantification of the proteins. This was confirmed using human plasma samples spiked with non-human protein standards in different concentrations.

Amongst all proteins identified in differentially regulated protein spots and peaks from OHSS+ FF samples after 2-DE and 2D LC fractionation were the proteins of the complement cascade and its regulatory proteins, several proteins involved in transport functions, as well as proteins regulating blood coagulation or participating in acute phase, inflammatory and immune responses. Several proteins participating in actin filament polymerization, regulation of angiogenesis and mineral balance were also identified. Three proteins, e.g. ceruloplasmin, kininogen-1 and complement C3 were shared between both

Table II The list of significantly different proteins identified (*P*-value of ≤0.05) between FF of OHSS+ and OHSS− selected using 2D LC.

Fraction No	Protein name	SwissProt No.	MW, kDa	pI	Up-regulation, fold change	Functionality
87	Alpha-1-antitrypsin	A1AT_HUMAN	47	5.4	OHSS+, 1.74	Acute-phase response
	Ceruloplasmin	CERU_HUMAN	122	5.4		Cellular iron ion homeostasis Copper ion transport Oxidation reduction
	Apolipoprotein A-I	APOA1_HUMAN	31	5.6		Cholesterol homeostasis
	Complement C3 precursor	CO3_HUMAN	187	6.0		Complement activation, alternative pathway Complement activation, classical pathway Positive regulation VEGF production
	Alpha-2-HS-glycoprotein	FETUA_HUMAN	39	5.4		Acute-phase response Regulation of inflammatory response
	Kininogen-1 precursor	KNG1_HUMAN	47	6.3		Blood coagulation Inflammatory response Negative regulation of blood coagulation Negative regulation of cell adhesion Vasodilation
265	Alpha-1-antitrypsin	A1AT_HUMAN	47	5.4	OHSS+, 1.79	Acute-phase response
	Ceruloplasmin	CERU_HUMAN	N	5.4		Cellular iron ion homeostasis Copper ion transport Oxidation reduction
268	Alpha-1-antitrypsin	A1AT_HUMAN	47	5.4	OHSS+, 1.67	Acute-phase response
	Ceruloplasmin	CERU_HUMAN	122	5.4		Cellular iron ion homeostasis Copper ion transport Oxidation reduction
	Alpha-2-HS-glycoprotein	FETUA_HUMAN	39	5.4		Acute-phase response Regulation of inflammatory response
270	Hemopexin	HEMO_HUMAN	52	6.6	OHSS+, 2.14	Cellular iron ion homeostasis Interspecies interaction between organisms
	Alpha-1B-glycoprotein precursor	A1BG_HUMAN	54	5.6		
	Serum albumin	ALBU_HUMAN	69	5.9		Cellular response to starvation Maintenance of mitochondrion location Negative regulation of apoptosis
952	Complement factor H-related protein 1	FHR1_HUMAN	38	7.8	OHSS+, 2.38	Complement activation
	Hepatocyte growth factor-like protein	HGFL_HUMAN	80	9.0		Blood coagulation Proteolysis

The table indicates band number, protein name, SwissProt No., predicted MW and pI, regulation/fold of the change and functionality based on search in UniProt/Gene Ontology/Biological Process.

proteomic approaches utilized in this study (Tables I and II) thus corroborating the validity of the findings.

Validation of proteomic data using western blotting

To confirm the results of 2D proteomic analyses, western blot experiments were performed for the following proteins: (i) highly elevated/significantly increased proteins in FF from OHSS+ patients: apolipoprotein A-IV with 2.2-fold change, ceruloplasmin reaching 2.3-fold change and alpha-2-HS-glycoprotein (fetuin-A) with 1.67 and 1.74-fold change; (ii) down-regulated kininogen-1 in OHSS+ patients by 2-DE (Table I), but present in protein peak up-regulated in OHSS+ FF samples according to 2D LC (Table II). In this protein peak kininogen-1 was identified as one of several unambiguously identified proteins from 2D LC with observed higher UV absorbance/protein level in OHSS+ FF. Such observations demonstrate a need for verification of such individual proteins from the overall pool of proteins identified.

In total, we used 23 FF samples (11 OHSS+ and 12 OHSS−) including 16 independent samples not previously used in proteomic

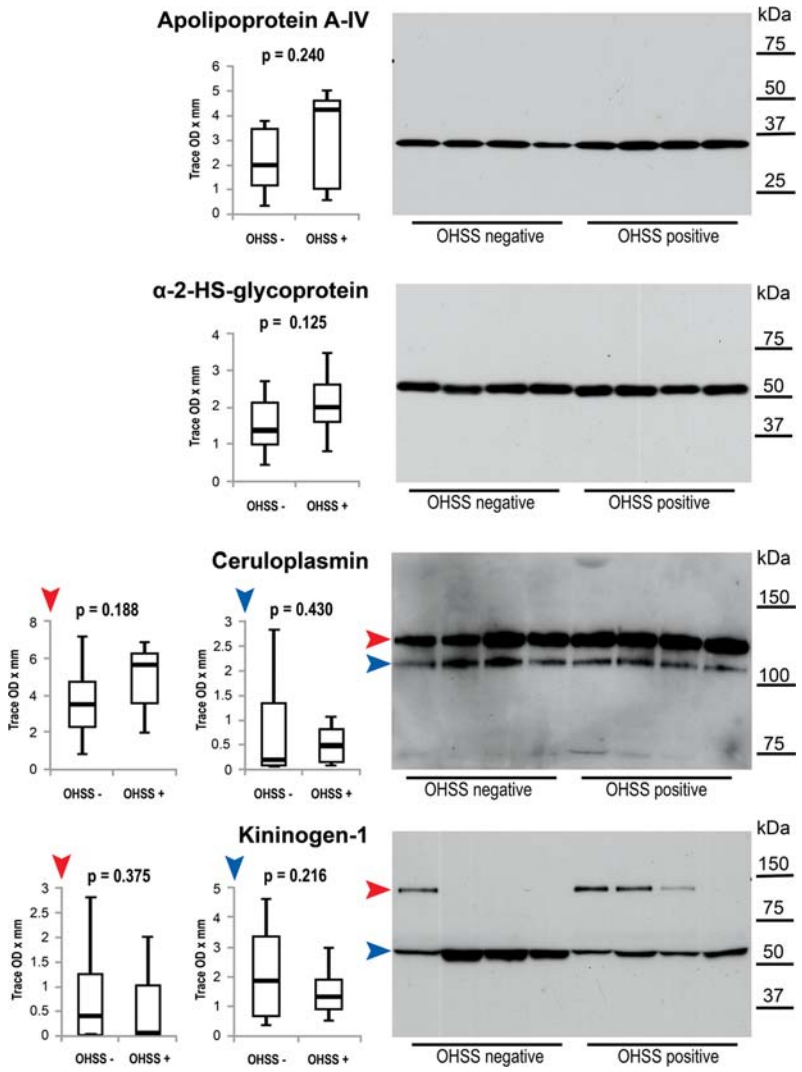

Figure 5 Immunoblot analysis of apolipoprotein A-IV, ceruloplasmin, alpha-2-HS-glycoprotein and kininogen-1 in samples of non-depleted FF of women undergoing IVF. Protein lysates prepared from samples of FF OFSS+ and OHSS− were examined on immunoblots using specific antibodies recognizing apolipoprotein A-IV, ceruloplasmin, alpha-2-HS-glycoprotein and kininogen-1. The protein bands were quantified using Quantity One software and distribution of the values was illustrated using box-plot. Significance of differences was calculated by Student *t*-test (*P*-value).

analyses. The non-depleted samples were separated using 1D SDS–PAGE followed by protein transfer and specific immunodetection. The representative results of 4 OHSS+ and 4 OHSS− samples of FF are shown in Fig. 5. The box-plots on the left side were created using optical density values for all 23 samples utilized in this study. The results demonstrated increase in the level of apolipoprotein A-IV, ceruloplasmin and apha-2-HS-glycoprotein in OHSS+ versus OHSS− FF samples whilst the level of kininogen-1 was lower in FF OHSS+ samples. Although the statistical evaluation did not find any significant differences at the level of *P*-value of ≤ 0.05, there was evident confirmation of the trends of protein changes observed by proteomic approaches with the probability varying from 57 to 88%. Many proteins present in fractionated spots or fractions may represent various forms (post-translationally modified, splicing variants, fragments etc.) of an individual protein. Hence, their possible quantitative differences found between samples may remain hidden or non-significant when detecting the total level of the same protein in the samples.

Computer modelling and simulation of possible interaction network connecting potential candidate proteins discriminating OHSS

Computer modelling techniques are very useful in examining the cellular pathways involved in maintaining the functions and cascades where many of the defined proteins may have a vital role to play. Identified proteins differentially regulated in FF from women undergoing IVF and suffering from severe form of OHSS (Protein/UniProt accession numbers provided in Table I) were introduced into a I2D

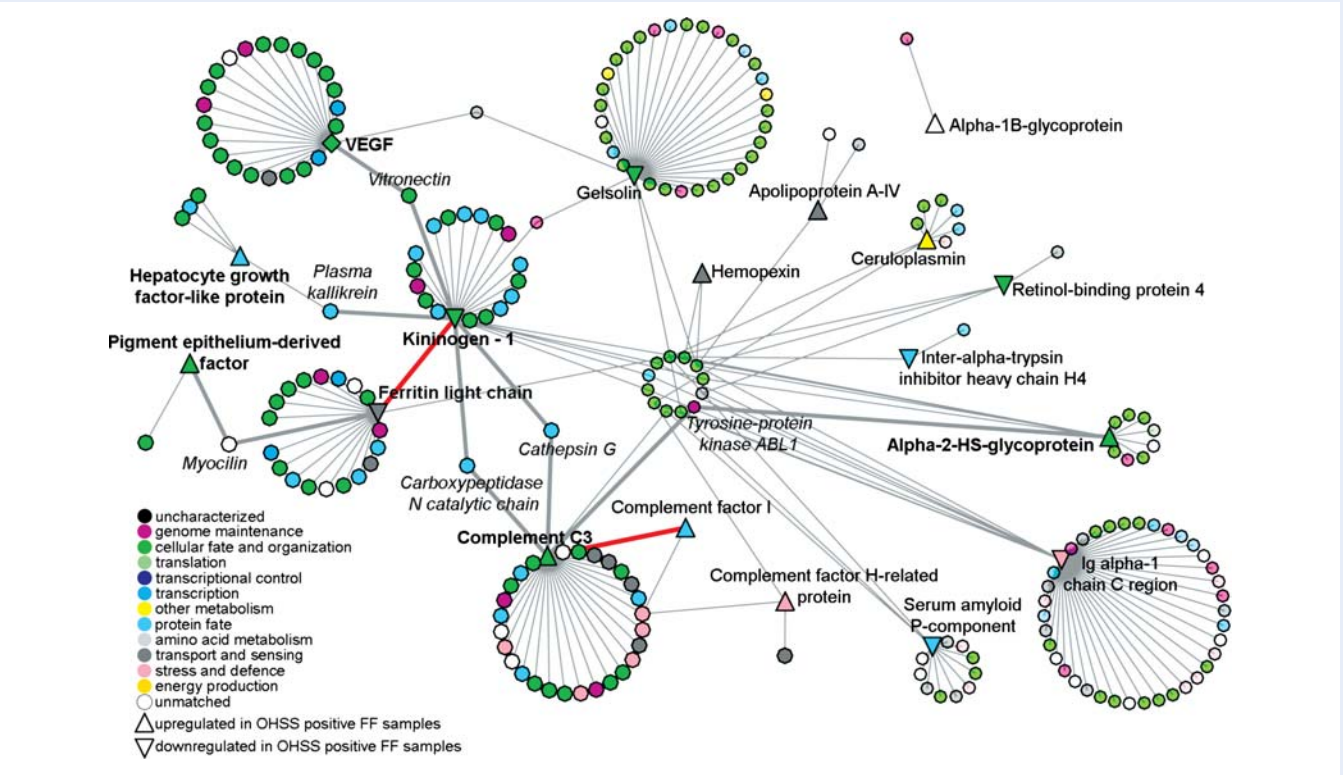

Figure 6 Computer modelling and simulation of possible interaction network connecting potential candidate proteins regulated during the development of severe OHSS. Network of possible protein–protein interactions, generated by querying I2D database and NAViGaTOR software for 16 identified proteins which were found to be regulated during the development of severe OHSS and VEGF. Some interacting proteins, with mediated interconnection are highlighted. Colour of nodes and edges represents Gene Ontology function.

database in order to identify possible interacting proteins and to construct protein–protein interaction networks enabling graphical visualization and possibly functional relationships amongst identified molecules (Fig. 6). The resulting interaction map contained in total 223 protein nodes and 240 interactions for the 16 proteins identified in this study and VEGF. Computer modelling highlighted the important role of kininogen-1 as an anchor for mediated interactions with other identified proteins such as complement C3 and Ig alpha-1 chain, VEGF, ferritin light chain and ceruloplasmin, hepatocyte growth factor-like protein as well as gelsolin, thus networking biological processes including inflammation and innate immunity, angiogenesis, iron transport and storage, blood coagulation and actin filament polymerization. The network revealed many other additional interacting proteins with possible role in OHSS, namely vitronectin (VTNC_HUMAN; P04004), cathepsin G (CATG_HUMAN; P08311) and carboxypeptidase N catalytic chain (CBPN_HUMAN; P15169), plasminogen (PLMN_HUMAN; P00747) and kallikrein (KLKB1_HUMAN, P03952). Contrary to the above, the apolipoprotoein A-IV (APOA4_HUMAN, P06727) and alpha-2-HS glycoprotein (FETUA_HUMAN, P02765; fetuin-A) remain segregated from this interaction network.

Discussion

A successful outcome from IVF depends on a preliminary phase of controlled ovarian hyperstimulation using exogenous gonadotrophins. The aim is to produce multiple follicles/oocytes without incurring the risk of OHSS. Currently, there is a lack of ability to predict success of the IVF treatment and better understanding of molecular processes might help increase IVF birth rate and at the same time avoid this life-threatening scenario which is associated with presence of inflammatory cytokines, neutrophil activation and increased capillary permeability (Orvieto, 2004; Orvieto *et al.*, 2006).

The milieu of FF is rich in hormones, growth factors, cytokines, anti-apoptotic factors, polysaccharides and various proteins which can give us a clue to the triggering of OHSS. Advances in -omics technologies, namely metabolomics and proteomics have helped immensely towards monitoring complex regulatory networks involved in ovarian physiology and responses to exogenous stimulation. Proteomic analyses of human FF identified a variety of proteins present in the FF and most of them were matched to plasma proteins (Spitzer *et al.*, 1996; Anahory *et al.*, 2002; Lee *et al.*, 2005; Angelucci *et al.*, 2006; Kim *et al.*, 2006; Schweigert *et al.*, 2006; Liu *et al.*, 2007; Hanrieder *et al.*, 2008; Estes *et al.*, 2009; Jarkovska *et al.*, 2010).

To our knowledge, this is the first study to date comparing the protein patterns of FF obtained from women suffering from severe form of OHSS and women with negligeble or mild symptoms of the disease. Our aim was to identify potential candidate proteins differentially represented in the two sample types used in our study and which may harbour parameters useful as 'handle' for identifying women at the risk of developing severe OHSS. Additionally, the interaction of

proteins might also help to increase our understanding of the molecular mechanisms involved in the progression of the disease. Firstly, we utilized an immunoaffinity system capable of removing 12 abundant blood plasma proteins and FF samples were processed using this system to remove plasma-matched follicular proteins. The proteins of flow-through fractions of FF were fractionated using a combination of two proteomic approaches and significant reproducible differences in protein composition of FF OFSS+ versus OHSS− were further analysed and identified by MS.

In summary, we identified a total of 19 candidate proteins differentially expressed between OHSS+ and OHSS− FF samples. Three proteins, namely ceruloplasmin, complement C3 and kininogen-1 were found using both 2D techniques. Several proteins including gelsolin, complement C3, serum amyloid P-component, ceruloplasmin and alpha-2-HS-glycoprotein were present in several protein spots or peaks with different pH indicating possible protein isoforms and/or post-translation modifications. In order to extrapolate both the functional interpretation as well as the validity of our proteomic findings, we utilized computer modelling to demonstrate that kininogen-1 may function as a key anchoring protein for other proteins participating in OHSS development and interacting with processes such as inflammation, angiogenesis, blood coagulation, iron transport and storage as well as innate immunity, cell adhesion and actin filament polymerization.

Kininogen-1 also known as high molecular weight kininogen (theoretical MW 72 kDa) is a multi-domain, multi-functional protein with middle concentration of around 80 μg/ml in plasma. It is known to play an important role in blood coagulation (Lalmanach *et al.*, 2010). Kininogen-1 is also a protein component of kallikrein–kinin system producing various mediators including mediators of inflammation and increased vascular permeability. The role of the kallikrein–kinin system in the pathophysiology of OHSS was suggested by Kobayashi *et al.* (1998) on the bases of the observation that OHSS ascites fluid caused microvascular hyperpermeability by a mechanism depending on kinin release. The association of the kinin–kallikrein system with the development of OHSS was also studied by Ujioka *et al.* (1998) on the rat model. Kallikrein cleaves kininogen-1 to pro-inflammatory kinins–bradykinin and cleaved kininogen. Bradykinin, in turn, is known to stimulate the release of mediators of pain and vascular dilation, whilst cleaved kininogen is involved in the release of elastase and superoxide. Importantly, cleaved kininogen induces release of pro-inflammatory cytokines TNF-α, IL-1β and IL-6 as well as chemokines IL-8 and MCP-1 from monocytes (Sainz *et al.*, 2007). Furthermore, computer simulation indicated that kallikrein may interact directly with hepatocyte growth factor-like protein, other protein differentially expressed in OHSS+ FF and also known as a macrophage stimulatory protein involved in macrophage activation (Suzuki *et al.*, 2008). Pro-inflammatory activities of bradykinin and cleaved kininogen are known to impact angiogenic activities and it is of interest that anti-angiogenic activity of cleaved kininogen can be blocked by binding ferritin (Coffman *et al.*, 2009; De Domenico *et al.*, 2009), thus allowing prevalence of pro-angiogenic activities of bradykinin and other molecules, which may subsequently lead to vessel formation (Coffman *et al.*, 2009). Ferritin, a direct binding partner of kininogen-1, similarly to cleaved kininogen, is recognized as an acute phase reactant and marker of both acute and chronic inflammation and known to increase in concentration 10–100-fold during inflammation (Coffman *et al.*, 2009). Another protein identified in our study was pigment epithelium-derived factor (PEDF), involved in inhibition of proliferation and cell migration of endothelial cells in ovaries (Cheung *et al.*, 2006). Recently, *in vivo* studies demonstrated anti-angiogenic properties of PEDF to inhibit VEGF mediated retina endothelial cell permeability through modulation of the Src kinase pathway (Sheikpranbabu *et al.*, 2010). Therefore, the tight regulation and direct or mediated interactions between the three proteins identified in this study, namely kininogen-1, ferritin and PEDF have strong implications in providing the balance between inflammatory process and angiogenesis, the two key processes that appear to be vital in the control of OHSS development. Taking into consideration the crucial role of VEGF in the increased endothelial/vessel permeability and development of OHSS, it was interesting to find an interconnecting link between VEGF and kininogen-1 mediated by vitronectin, a cell adhesion and spreading factor, thus confirming the role of cell adhesion proteins in the control of the angiogenesis in this study. Recent advances due to *in vitro* human cell co-culture model have successfully managed to show the paracrine effect of hCG on increase endothelial permeability by up-regulating VEGF in luteinized granulosa cells. This causes reduction of membrane-bound adhesion protein claudin 5 and impacts endothelial permeability (Rodewald *et al.*, 2009). In addition to the processes mentioned above that appear to play a central role in the development of severe OHSS, we also observed a relationship between kininogen-1 and complement component C3 mediated by cathepsin G and carboxypeptidase N catalytic chain. This provided a clear indication that the role of kininogen-1 and its associated processes can be extended to the control of innate immunity mediated by complement cascade. Whilst inhibition of complement activity in FF of women undergoing controlled ovarian hyperstimulation for IVF is critical in physiological folliculogenesis (Jarkovska *et al.*, 2010), it also appears to be implicated in the development of severe OHSS.

Additionally, we identified two other proteins in our study that were sequestered out of the above described network: apolipoprotein A-IV and alpha-2-HS-glycoprotein (fetuin-A). Apoa-IV is a major component of high density lipoprotein and chylomicron involved in lipid transportation. The regulation of this protein associated with the development of severe OHSS observed in this study indicated that lipid metabolism may be closely related to reproductive processes. Alpha-2-HS-glycoprotein (fetuin-A), a low abundant protein with normal levels in serum reaching around 300–600 pg/ml, is known to decrease during inflammation. Interestingly, inflammation itself stimulates the release of anti-inflammatory mediators, such as IL-10, steroids and spermine which in turn leads to activation of the acute phase response and decrease in fetuin-A level (Ombrellino *et al.*, 2001). Based on our finding of decreased level of kininogen-1, ferritin, and increased level of fetuin-A in severe OHSS+ women, we postulate that such changes are part of a counter-balancing response to the inflammatory process, which if not controlled, can have a detrimental effect on the patient and the therapy outcome.

Looking at the molecular processes underlying the pathogenesis of OHSS, the central role of inflammation and its tight link to angiogenesis was very evident. Furthermore, the contributions from innate immunity, transport mechanisms and cell adhesion played a significant part too. Biological variability is a common challenge in any study using limited number of patient samples in such discovery-related proteomic analyses because patient variability can simply lower or mask

many important qualitative and quantitative differences. Additionally, it is important to consider that not only do quantitative protein changes play an important role, but also that there may be various other parameters such as truncation and post-translational modification(s) of selected proteins impacting the overall picture. Hence, a combined group of several biomarkers would be more beneficial and reliable than a single protein as marker or indicator of the disease process and its onset. In this study, we propose a set of key proteins as potential biomarker candidates useful in the prognosis/diagnosis of the development of severe OHSS and for monitoring IVF therapy.

Larger, preferably multicentric joint collaborative studies on patient groups are necessary to confirm our findings. Hopefully, any positive outcome of such studies should advance our understanding of the processes involved in the onset of OHSS, as well as provide a direction for novel therapeutic interventions.

Supplementary data

Supplementary data are available at http://molehr.oxfordjournals.org/.

Authors' roles

H.K., J.M. and S.J.G. were responsible for the conception and design of this study. K.R. performed the sample collection and clinical data acquisition. K.J., H.K.S. and R.H. carried out the electrophoretic and liquid chromatography experiments whilst P.H. identified the differentially expressed proteins. The proteomic data were analysed and interpreted by K.J., R.H. and H.K.; K.J., P.H., R.H., J.M., K.R. contributed to drafting of the article and H.K.S., S.J.G. and H.K. critically revised the manuscript. All of the authors contributed to the final approval of the manuscript for publication.

Acknowledgements

Special thanks to A. Ekefjärd and D. Enetoft from Ludesi for providing Viper software.

Conflict of interest

With the recent acquisition of Millipore by Merck GmbH, and the usage of several biologicals for this study from previously Millipore (now Merck Millipore Bioscience) as well as Sigma Aldrich, all authors see no conflict of Interest. None of these companies had any other participating interests in this study. All participating authors declare that they have no competing interests.

Funding

This research was supported by Ministry of Health of the Czech Republic (NS9781-32009), and Institutional Research Concepts AV0Z50450515 (IAPG), AV0Z50200510 (IMIC).

References

Albert C, Garrido N, Mercader A, Rao CV, Remohi J, Simon C, Pellicer A. The role of endothelial cells in the pathogenesis of ovarian hyperstimulation syndrome. *Mol Hum Reprod* 2002;**8**:409–418.

Anahory T, Dechaud H, Bennes R, Marin P, Lamb NJ, Laoudj D. Identification of new proteins in follicular fluid of mature human follicles. *Electrophoresis* 2002;**23**:1197–1202.

Andersen AN, Goossens V, Bhattacharya S, Ferraretti AP, Kupka MS, de Mouzon J, Nygren KG. Assisted reproductive technology and intrauterine inseminations in Europe, 2005: results generated from European registers by ESHRE: ESHRE. The European IVF Monitoring Programme (EIM), for the European Society of Human Reproduction and Embryology (ESHRE). *Hum Reprod* 2009;**24**:1267–1287.

Angelucci S, Ciavardelli D, Di Giuseppe F, Eleuterio E, Sulpizio M, Tiboni GM, Giampietro F, Palumbo P, Di Ilio C. Proteome analysis of human follicular fluid. *Biochim Biophys Acta (BBA) - Proteins Proteomics* 2006;**1764**:1775–1785.

Boivin J, Bunting L, Collins JA, Nygren KG. International estimates of infertility prevalence and treatment-seeking: potential need and demand for infertility medical care. *Hum Reprod* 2007;**22**:1506–1512.

Chen SU, Chen CD, Yang YS. Ovarian hyperstimulation syndrome (OHSS): new strategies of prevention and treatment. *J Formos Med Assoc* 2008;**107**:509–512.

Chen SU, Chou CH, Lin CW, Lee H, Wu JC, Lu HF, Chen CD, Yang YS. Signal mechanisms of vascular endothelial growth factor and interleukin-8 in ovarian hyperstimulation syndrome: dopamine targets their common pathways. *Hum Reprod* 2010;**25**:757–767.

Cheung LW, Au SC, Cheung AN, Ngan HY, Tombran-Tink J, Auersperg N, Wong AS. Pigment epithelium-derived factor is estrogen sensitive and inhibits the growth of human ovarian cancer and ovarian surface epithelial cells. *Endocrinology* 2006;**147**:4179–4191.

Chipwete SE, Bugren S, Rafla N. Thrombosis post ovarian hyperstimulation. *Fertil Steril* 2009;**91**:1956.e13–1956.e14.

Coffman LG, Parsonage D, D'Agostino R Jr, Torti FM, Torti SV. Regulatory effects of ferritin on angiogenesis. *Proc Natl Acad Sci USA* 2009;**106**:570–575.

De Domenico I, Ward DM, Kaplan J. Serum ferritin regulates blood vessel formation: a role beyond iron storage. *Proc Natl Acad Sci USA* 2009;**106**:1683–1684.

de Mouzon J, Goossens V, Bhattacharya S, Castilla JA, Ferraretti AP, Korsak V, Kupka M, Nygren KG, Nyboe Andersen A; The European Ivf-monitoring Consortium ftESoHR. Assisted reproductive technology in Europe, 2006: results generated from European registers by ESHRE. *Hum Reprod* 2010;**25**:1851–1862.

Estes SJ, Ye B, Qiu W, Cramer D, Hornstein MD, Missmer SA. A proteomic analysis of IVF follicular fluid in women ≤32 years old. *Fertil Steril* 2009;**92**:1569–1578.

Fortune JE. Ovarian follicular growth and development in mammals. *Biol Reprod* 1994;**50**:225–232.

Gadher SJ, Jarkovska K, Kovarova H. Reproductive therapies and a need for potential biomarkers for prognostic and diagnostic screening of women desperate to conceive. *Expert Rev Proteomics* 2009;**6**:591–593.

Gerris J, Delvinge A, Olivennes F. *Ovarian Hyperstimulation Syndrome*. London, UK: Informa Healthcare, 2006.

Hanrieder J, Nyakas A, Naessen T, Bergquist J. Proteomic analysis of human follicular fluid using an alternative bottom-up approach. *J Proteome Res* 2008;**7**:443–449.

Huang L, Harvie G, Feitelson JS, Gramatikoff K, Herold DA, Allen DL, Amunngama R, Hagler RA, Pisano MR, Zhang WW *et al.* Immunoaffinity separation of plasma proteins by IgY microbeads: meeting the needs of proteomic sample preparation and analysis. *Proteomics* 2005;**5**:3314–3328.

Jarkovska K, Martinkova J, Liskova L, Halada P, Moos J, Rezabek K, Gadher SJ, Kovarova H. Proteome mining of human follicular fluid

reveals a crucial role of complement cascade and key biological pathways in women undergoing in vitro fertilization. *J Proteome Res* 2010;**9**:1289–1301.

Kim YS, Kim MS, Lee SH, Choi BC, Lim JM, Cha KY, Baek KH. Proteomic analysis of recurrent spontaneous abortion: identification of an inadequately expressed set of proteins in human follicular fluid. *Proteomics* 2006;**6**:3445–3454.

Kobayashi H, Okada Y, Asahina T, Gotoh J, Terao T. The kallikrein-kinin system, but not vascular endothelial growth factor, plays a role in the increased vascular permeability associated with ovarian hyperstimulation syndrome. *J Mol Endocrinol* 1998;**20**:363–374.

Lalmanach G, Naudin C, Lecaille F, Fritz H. Kininogens: More than cysteine protease inhibitors and kinin precursors. *Biochimie* 2010;**92**:1568–1579.

Lee HC, Lee SW, Lee KW, Cha KY, Kim KH, Lee S. Identification of new proteins in follicular fluid from mature human follicles by direct sample rehydration method of two-dimensional polyacrylamide gel electrophoresis. *J Korean Med Sci* 2005;**20**:456–460.

Lei ZM, Reshef E, Rao V. The expression of human chorionic gonadotropin/luteinizing hormone receptors in human endometrial and myometrial blood vessels. *J Clin Endocrinol Metab* 1992;**75**:651–659.

Liu T, Qian WJ, Mottaz HM, Gritsenko MA, Norbeck AD, Moore RJ, Purvine SO, Camp DG 2nd, Smith RD. Evaluation of multiprotein immunoaffinity subtraction for plasma proteomics and candidate biomarker discovery using mass spectrometry. *Mol Cell Proteomics* 2006;**5**:2167–2174.

Liu AX, Zhu YM, Luo Q, Wu YT, Gao HJ, Zhu XM, Xu CM, Huang HF. Specific peptide patterns of follicular fluids at different growth stages analyzed by matrix-assisted laser desorption/ionization time-of-flight mass spectrometry. *Biochim Biophys Acta* 2007;**1770**:29–38.

Merrilees DA, Kennedy-Smith A, Robinson RG. Obstructive uropathy as the etiology of renal failure in ovarian hyperstimulation syndrome. *Fertil Steril* 2008;**89**:992e991–992.

Moos J, Filova V, Pavelkova J, Moosova M, Peknicova J, Rezabek K. Follicular fluid and serum levels of inhibin A and pregnancy-associated plasma protein A in patients undergoing IVF. *Fertil Steril* 2009;**91**:1739–1744.

Nastri CO, Ferriani RA, Rocha IA, Martins WP. Ovarian hyperstimulation syndrome: pathophysiology and prevention. *J Assist Reprod Genet* 2010;**27**:121–128.

Navot D, Bergh PA, Laufer N. Ovarian hyperstimulation syndrome in novel reproductive technologies: prevention and treatment. *Fertil Steril* 1992;**58**:249–261.

Ombrellino M, Wang H, Yang H, Zhang M, Vishnubhakat J, Frazier A, Scher LA, Friedman SG, Tracey KJ. Fetuin, a negative acute phase protein, attenuates TNF synthesis and the innate inflammatory response to carrageenan. *Shock* 2001;**15**:181–185.

Orvieto R. Controlled ovarian hyperstimulation—an inflammatory state. *J Soc Gynecol Investig* 2004;**11**:424–426.

Orvieto R, Zagatsky I, Yulzari-Roll V, La Marca A, Fisch B. Substituting human chorionic gonadotropin by gonadotropin-releasing hormone agonist to trigger final follicular maturation, during controlled ovarian hyperstimulation, results in less systemic inflammation. *Gynecol Endocrinol* 2006;**22**:437–440.

Rao CV, Li X, Toth P, Lei ZM, Cook VD. Novel expression of functional human chorionic gonadotropin/luteinizing hormone receptor gene in human umbilical cords. *J Clin Endocrinol Metab* 1993;**77**:1706–1714.

Rodewald M, Herr D, Duncan WC, Fraser HM, Hack G, Konrad R, Gagsteiger F, Kreienberg R, Wulff C. Molecular mechanisms of ovarian hyperstimulation syndrome: paracrine reduction of endothelial claudin 5 by hCG in vitro is associated with increased endothelial permeability. *Hum Reprod* 2009;**24**:1191–1199.

Sainz IM, Pixley RA, Colman RW. Fifty years of research on the plasma kallikrein-kinin system: from protein structure and function to cell biology and in-vivo pathophysiology. *Thromb Haemost* 2007;**98**:77–83.

Schweigert FJ, Gericke B, Wolfram W, Kaisers U, Dudenhausen JW. Peptide and protein profiles in serum and follicular fluid of women undergoing IVF. *Hum Reprod* 2006;**21**:2960–2968.

Shalgi R, Kraicer P, Rimon A, Pinto M, Soferman N. Proteins of human follicular fluid: the blood-follicle barrier. *Fertil Steril* 1973;**24**:429–434.

Sheikpranbabu S, Ravinarayanan H, Elayappan B, Jongsun P, Gurunathan S. Pigment epithelium-derived factor inhibits vascular endothelial growth factor-and interleukin-1beta-induced vascular permeability and angiogenesis in retinal endothelial cells. *Vascul Pharmacol* 2010;**52**:84–94.

Shevchenko A, Wilm M, Vorm O, Mann M. Mass spectrometric sequencing of proteins silver-stained polyacrylamide gels. *Anal Chem* 1996;**68**:850–858.

Spitzer D, Murach KF, Lottspeich F, Staudach A, Illmensee K. Different protein patterns derived from follicular fluid of mature and immature human follicles. *Hum Reprod* 1996;**11**:798–807.

Suzuki Y, Funakoshi H, Machide M, Matsumoto K, Nakamura T. Regulation of cell migration and cytokine production by HGF-like protein (HLP)/macrophage stimulating protein (MSP) in primary microglia. *Biomed Res* 2008;**29**:77–84.

Ujioka T, Matsuura K, Tanaka N, Okamura H. Involvement of ovarian kinin-kallikrein system in the pathophysiology of ovarian hyperstimulation syndrome: studies in a rat model. *Hum Reprod* 1998;**13**:3009–3015.

Wulff C, Wilson H, Largue P, Duncan WC, Armstrong DG, Fraser HM. Angiogenesis in the human corpus luteum: localization and changes in angiopoietins, tie-2, and vascular endothelial growth factor messenger ribonucleic acid. *J Clin Endocrinol Metab* 2000;**85**:4302–4309.